Original Article

Assessment of a 2D electronic portal imaging devices-based dosimetry algorithm for pretreatment and *in-vivo* midplane dose verification

Ali Jomehzadeh[1,2,3], Parvaneh Shokrani[1], Mohammad Mohammadi[4], Alireza Amouheidari[5]

[1]Department of Medical Physics, School of Medicine, Isfahan University of Medical Sciences, Isfahan, [2]Department of Medical Physics, School of Medicine, Rafsanjan University of Medical Sciences, Rafsanjan, [3]Department of Medical Physics, School of Medicine, Hamadan University of Medical Sciences, Hamadan, [4]Department of Radiation Oncology, Isfahan Milad Hospital, Isfahan, Iran, [5]Department of Radiation Oncology, The Netherlands Cancer Institute, Amsterdam, The Netherlands

Abstract

Background: The use of electronic portal imaging devices (EPIDs) is a method for the dosimetric verification of radiotherapy plans, both pretreatment and *in vivo*. The aim of this study is to test a 2D EPID-based dosimetry algorithm for dose verification of some plans inside a homogenous and anthropomorphic phantom and *in vivo* as well.

Materials and Methods: Dose distributions were reconstructed from EPID images using a 2D EPID dosimetry algorithm inside a homogenous slab phantom for a simple 10 × 10 cm^2 box technique, 3D conformal (prostate, head-and-neck, and lung), and intensity-modulated radiation therapy (IMRT) prostate plans inside an anthropomorphic (Alderson) phantom and in the patients (one fraction *in vivo*) for 3D conformal plans (prostate, head-and-neck and lung).

Results: The planned and EPID dose difference at the isocenter, on an average, was 1.7% for pretreatment verification and less than 3% for all *in vivo* plans, except for head-and-neck, which was 3.6%. The mean γ values for a seven-field prostate IMRT plan delivered to the Alderson phantom varied from 0.28 to 0.65. For 3D conformal plans applied for the Alderson phantom, all γ1% values were within the tolerance level for all plans and in both anteroposterior and posteroanterior (AP-PA) beams.

Conclusion: The 2D EPID-based dosimetry algorithm provides an accurate method to verify the dose of a simple 10 × 10 cm^2 field, in two dimensions, inside a homogenous slab phantom and an IMRT prostate plan, as well as in 3D conformal plans (prostate, head-and-neck, and lung plans) applied using an anthropomorphic phantom and *in vivo*. However, further investigation to improve the 2D EPID dosimetry algorithm for a head-and-neck case, is necessary.

Key Words: Algorithm, electronic portal imaging devices dosimetry, *in vivo* dosimetry, midplane, pretreatment verification

Address for correspondence:
Dr. Parvaneh Shokrani, Department of Medical Physics, School of Medicine, Isfahan University of Medical Sciences, Isfahan, Iran.
E-mail: shokrani@med.mui.ac.ir
Received: 16.03.2014, Accepted: 12.05.2014

Access this article online	
Quick Response Code:	Website: www.advbiores.net
	DOI: 10.4103/2277-9175.194799

INTRODUCTION

As the complexity of the radiotherapy process increases, the need for verification of accuracy of the

How to cite this article: Jomehzadeh A, Shokrani P, Mohammadi M, Amouheidari A. Assessment of a 2D electronic portal imaging devices-based dosimetry algorithm for pretreatment and *in-vivo* midplane dose verification. Adv Biomed Res 2016;5:171.

dose delivered becomes more important. Image-guided radiotherapy (IGRT) tools have been made available by vendors for geometric verification of patient positioning. In addition, verification of the dose, either pretreatment or *in vivo,* plays an important part for a quality assurance program for advanced irradiation techniques. The importance of pretreatment or *in vivo* verification of the dose delivered to the patient has also been increased; due to the increasing complexity of the new radiotherapy techniques.[1-4] Pretreatment verification is a commonly used substitute method, whereby, the planned dose is verified before treatment. In pretreatment, various treatment parameters, including the beam energy, number of monitor units, and multileaf collimator (MLC) settings, have to be verified, to ensure an accurate dose delivered to a patient. The above parameters can be used to calculate dose distribution within a homogenous phantom. The drawback, however, is, those errors occurring at the time of treatment cannot be detected and it is not clear how errors detected in pretreatment would translate to errors within a patient. Ideal dose delivery at radiotherapy, especially *in vivo,* is an alternative that ensures that the dose distribution delivered to the patient at the time of treatment corresponds to the planned treatment.[5]

Portal images acquired by using EPIDs have been addressed as a key element for the above-mentioned verifications.[4,6-17] EPIDs are convenient tools for both pretreatment verification and *in vivo* dosimetry.[5,14,18] An EPID image is converted to a pretreatment or *in vivo* dose distribution (with a phantom or patient) using an appropriate approach verification of the dose calculation and plan deliverability.

A dose verification method based on an EPID and using a back-projection approach has been developed at the Netherlands Cancer Institute-Antoni van Leeuwenhoek (NKI-AVL). Two-dimensional dose distributions inside a phantom or patient are reconstructed from portal images using the back-projection algorithm. The model requires the primary dose component at the position of the EPID. A parameterized description of the lateral scatter within the imager is obtained from measurements with an ionization chamber in a mini phantom. It is currently used for all IMRT treatments, preferably for *in vivo* or otherwise for pretreatment verification. The midline dose can be determined by converting the measured entrance (or exit) dose with the depth dose data, taking the inhomogeneities into account.[19-22] However, the drawbacks of these methods are that additional patient information is required to determine the midline dose, and the measurements and calculations are not completely independent of the treatment planning process.[23] The back-projection approach is a method to derive the midplane dose from the transmission dose data measured with an EPID, without additional patient information, that is, independent of a treatment planning system (TPS).[23]

Several articles have reported pretreatment and *in vivo* EPID-based dosimetry for IMRT plans based on the determined midplane dose. Boellard *et al*.[23] developed a new method to derive the midplane dose from the transmission dose data, measured with a scanning liquid ionization chamber (SLIC) EPID, which is not the commercialized and tested transmission dose method to obtain the midline dose in homogenous and symmetrical inhomogeneous phantoms. Wendling *et al*.[5] modified a previously developed EPID back-projection algorithm, but just for prostate IMRT treatments and applied it to an amorphous silicon EPID. McDermott *et al*.[15] investigated the feasibility of replacing pretreatment verification with *in vivo* EPID dosimetry for only prostate IMRT plans. To our knowledge, to date, an amorphous silicon (a-Si) EPID has not been employed to determine the midplane dose using an Anthropomorphic (Alderson) phantom with inhomogenities.

In this study, we assay a 2D EPID-based dosimetry algorithm to compare the reconstructed dose distributions with the corresponding TPS calculated dose distributions for a simple 10 × 10 cm^2 box technique, IMRT prostate, and 3D conformal plans (head-and-neck, prostate, and lung), using a homogenous slab and anthropomorphic (Alderson) phantoms, and also inside a patient *(in vivo)* for three conformal plans (prostate, head-and-neck, and lung).

MATERIALS AND METHODS

Accelerator and electronic portal imaging devices

In this study measurements were performed in the Department of Radiation Oncology of the Netherlands cancer institute on various SL20i linear accelerators (Elekta, Crawley, U.K) using 10 MV and 6 MV photon beams for prostate, lung, and head-and-neck plans. All accelerators are equipped with a multileaf collimator (MLC), consisting of 40 leaf pairs with a projected leaf width of 1 cm at the isocenter.[24] A PerkinElmer RID 1680 AL5/Elekta IView GT a-Si EPID was used for all the measurements. The EPID has an intrinsic 1 mm thick copper plate on top of the scintillation layer. An extra 2.5 mm thick copper plate was mounted directly on top of the standard plate, both as an additional buildup material and to absorb the scattered low-energy photons from the phantom or patient.[25] The sensitive area of the EPID is 41 × 41 cm^2. Images were acquired using an in-house developed software.[25,26]

Electronic portal imaging devices-based dosimetry using a back-projection algorithm

Images were acquired with an amorphous silicon flat panel imager. Details regarding the image acquisition, stability, imager design, and dosimetric characteristics have been reported extensively in literature.[25,26] The details of the algorithm used to determine dose images within a patient (or phantom) for the present study has also been described elsewhere,[5,23] and will be briefly outlined here. The algorithm converts segment images to a 2D distribution of absolute dose in the reconstruction plane of the patient, defined as the plane perpendicular to the beam axis.[5,27,28] Therefore, this plane rotates with the gantry. The pixel values of the transit dose image are processed using scatter kernels (for scatter produced within the EPID and inside the patient reaching the EPID), the scatter-to-primary ratio (for scattered radiation within the patient), the inverse square law factor, and the measured transmission factor, to obtain absolute dose distribution in the isocentric plane of the patient. The measured transmission of the beam through the patient is determined from images acquired for segments of each field both with and without the patient. The location of the reconstruction plane is arbitrary, so a correction is required to account for attenuation of the beam from the isocentric plane to the exit surface. The external contour of the patient's computed tomography (CT) scan is used to obtain the ratio of the geometrical path lengths, which is used to calculate the attenuation per pixel. Reconstructed 2D dose distributions for each field are then the sum of the reconstructed dose distributions of all the segments belonging to that field.

Treatment planning and dose comparison

Dose distributions were calculated with the current clinical version of the TPS (Pinnacle V9.0, Philips Medical Systems, Eindhoven, the Netherlands). All dose distributions were calculated using Pinnacle's adaptive convolution/superposition approach. This was a fast implementation of the collapsed cone convolution/superposition algorithm and included an advanced tissue inhomogeneity correction.[29] Dose distributions reconstructed from EPID images were compared with the planned dose distributions using 2D γ evaluation within the 20% isodose line for the conformal plans and the IMRT cases. The 20% isodose surface was chosen to improve the γ-statistics and masked regions with discrepancies.[15] The following criteria were used for gamma statistics — a dose difference tolerance of 3% and a distance-to-agreement tolerance of 3 mm. An EPID dosimetry report was created for each treatment plan, providing for each beam the mean γ,"the near maximum γ value" γ1%, and the percentage of points with $\gamma \leq 1$ ($P^{\gamma} \leq_1$ or pass rate), as well as the dose at the isocenter. A green dot in the EPID dosimetry report meant that all alert criteria were within tolerance level ($\gamma_{mean} \leq 0.5$, $\gamma_{1\%} \leq 2$, $P^{\gamma} \leq_1 \geq 85\%$and $\Delta D_{isoc} \leq 3\%$). The yellow dot in the report indicated that at least one of the alert criteria was outside the tolerance level, but still within the action level ($0.5 \leq \gamma_{mean} < 1.0$, $2 \leq \gamma_{1\%} < 4$, $70\% \leq P^{\gamma} \leq 1 < 85\%$ and $3\% \leq \Delta D_{isoc} < 5\%$). The red dot indicated that at least for one of the evaluation criteria the error was outside the action level ($\gamma_{mean} > 1$, $\gamma_{1\%} > 4$, $P^{\gamma} \leq 1 < 70\%$ and $\Delta D_{isoc} > 5\%$).

Dose verification in the phantoms and the patients

In order to assay the 2D EPID-based dosimetry algorithm, measurements were performed using a homogenous polystyrene phantom (slab phantom of 30 × 30 cm^2 area and 20 cm height) and an inhomogeneous anthropomorphic (Alderson) phantom — the former being a more realistic approximation of clinical situations. The Alderson phantom was positioned in a supine position and the three conformal plans (prostate, head-and-neck, and lung) and one seven-field IMRT prostate plan were randomly selected. The plans were recalculated with the TPS, replacing the patient planning CT scan with a phantom CT scan using the same plan parameters — the MLC settings, gantry, and collimator angles, numbers of monitor units and energy. In the case of homogenous slab phantom measurements, the phantom was irradiated with a simple box technique (four-field, 10 × 10 cm^2, 10 MV). The source surface distance (SSD) was 90 cm at a gantry angle of 0° and the isocenter was positioned at the middle of the phantom. For all measurements the source-to-imager distance (SID) was 150 cm.

In vivo EPID dose verification was performed for the same fractions as setup verification for prostate, head-and-neck, and lung plans. Additional EPID dosimetry images were acquired at the third fraction to ensure five *in vivo* measurements within the first two weeks plus one day of treatment. Therefore, EPID treatment images were acquired at the first three fractions and then once per week, as also for any fractions requiring an additional setup verification. The first measured fraction for each patient was included in this study. Plans were first compared at the isocenter, by summing the planned and EPID isocenter doses for each field, respectively. Each field was then compared in 2D at the plane corresponding to the location of the reconstructed dose distribution determined with the EPID.

RESULTS

Phantom measurements

Homogenous slab phantom (pretreatment verification)

The results of the γ-evaluation for a simple box configuration delivered to a slab phantom analyzed with the 2D midplane EPID dosimetry approach are shown in Figure 1. Within the area of the 20% isodose lines, the percentage of points with $\gamma \leq 1$ for all fields is within the tolerance level. The average pass rate is 96.3 ± 3.1%, which also shows good agreement.

In Table 1 the average results (1SD) of the γ-evaluation parameters (mean γ and γ1%) and dose difference at isocenter for the simple box field with the slab phantom are presented. For the simple fields, all γ-evaluation parameters and dose difference at the isocenter are within the tolerance level. The mean γ and $\gamma_{1\%}$ values averaged over the four simple fields are 0.4±0.11 (1SD) and 1.0 ± 0.1, respectively. All γ distributions had mean γ and $\gamma_{1\%}$ values below 0.48 and 1.1, respectively. The AP beam (gantry angle of 0°) had the highest γ values, including mean γ, γ1%, and dose difference at the isocenter with respect to the PA beam. The measured dose at the isocenter was 1.8% below the planned dose, which was within the tolerance level for the mentioned criterion. The individual measured fields were compared and had very good agreement with the planned dose distributions achieved.

In Figure 2 a set of planned X and Y dose profiles is compared with the measured ones acquired from the reconstructed EPID midplane dose image of a slab phantom, which demonstrate very good agreement, especially in the penumbra region. The EPID reconstructed dose on the central axis is 1.8% below the planned dose.

Alderson phantom

In Figure 3 the mean γ, γ1%, and the measured and planned dose values of the three delivered clinical conformal plans (head-and-neck, lung, and prostate) in an Alderson phantom are presented, using the AP–PA beams. For the lung plan, the mean γ on anterior–posterior (AP) beam is 12.2%, larger than the tolerance level and in the posterior–anterior (PA) beam. The head-and-neck plan has a larger mean γ value (10.7%) than the tolerance level, while all γ1% values are within the tolerance level for all plans in both AP and PA beams. The lung plan has the highest mean γ for the AP beam, while on the PA beam the head-and-neck has the highest mean. Figure 3b indicates that the planned dose for the AP beam is higher than the EPID reconstructed dose for all plans, while for the PA beam it is the opposite.

Figure 4 represents the percentage of points with $\gamma \leq 1$, within the area of the 20% isodose lines for the three conformal plans in the Alderson phantom. Figure 4a shows the γ1% of both the AP–PA beams for the conformal plans and Figure 4b represents the γ1% values of a seven-field prostate IMRT plan, field by field: The percentage of points with $\gamma \leq 1$ are 5.3, 10.2, 7.5, and 7.0% larger than the tolerance level, respectively.

In Figure 5 the mean γ and γ1% values of the seven-field prostate IMRT delivered clinical plan in the Alderson phantom is presented. The mean γ values varied between 0.28 and 0.65. Figure 5 also shows that the γ1% for all fields is less than 2 (the tolerance level). The gantry angle of 150° had the highest γ failure rate for both mean γ and γ1%.

Patient measurements

The example presented in Figure 6 is one fraction of an *in vivo* verification EPID dosimetry reported for three-dimensional conformal plans, including prostate, lung, and head-and-neck cancer treatments. The dose distributions reconstructed by the 2D

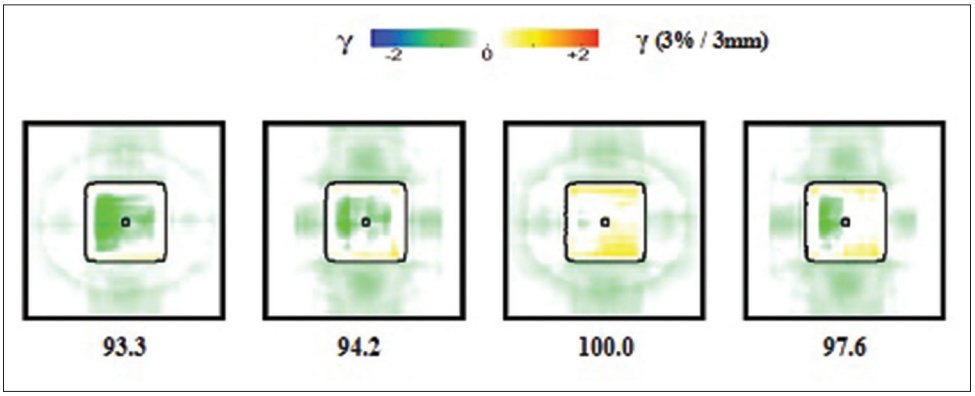

Figure 1: γ-evaluation of a four-field box plan using 2D EPID reconstruction through a homogenous slab phantom. The percentage of $\gamma \leq 1$ within the 20% isodose line for each field is given at the bottom of figures

EPID dosimetry algorithm were compared with the planned dose distributions. The difference between the measured and planned doses at the isocenter was less than 3% for all plans except for the head-and-neck plan, which was 16.7%. The mean γ value for all plans was less than 0.5 except for one field (G = 120°), which was about 18% higher than the tolerance level and a warning was raised. On an average, over all fields, the mean γ value was found to be 0.41 for all plans. Within the area of the 20% isodose lines, the near maximum γ value averaged over all fields was 1.20, 1.27, and 1.56 for the prostate, lung, and head-and-neck plans, respectively.

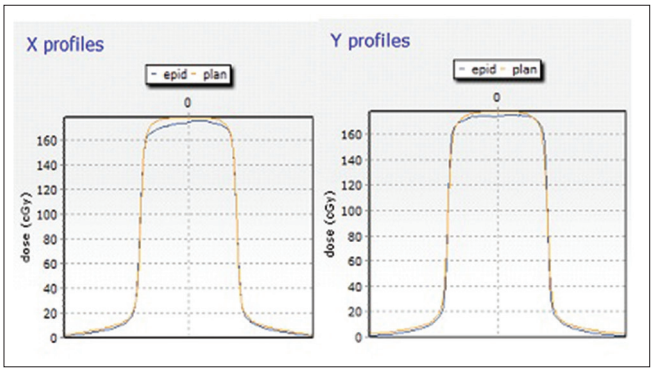

Figure 2: Absolute dose profiles of a square field (G = 0°) reconstructed by EPID in the midplane (blue curve) and calculated by the TPS (red curve)

DISCUSSION

For the inhomogenous phantom dose verification, the dose distributions resulting from the EPID

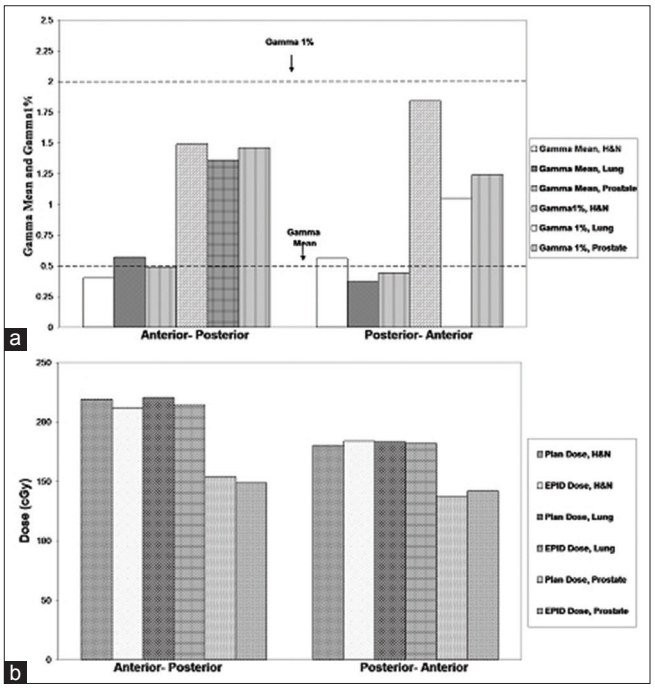

Figure 3: The results of (a) γ mean and γ1% and (b) planned and EPID doses for both beam directions, of the prostate, head-and-neck, and lung plans with the Alderson phantom. The dashed lines indicate the tolerance level for Figure 3a

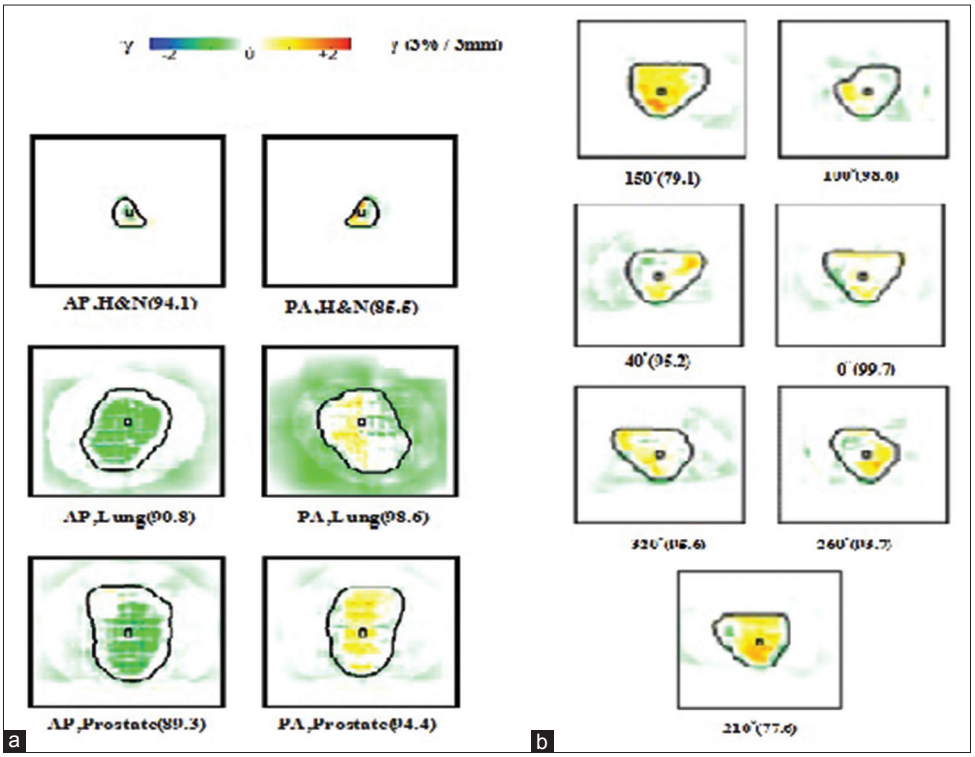

Figure 4: γ-evaluation of (a) the head-and-neck, lung, and prostate plans for both AP–PA beams and (b) a seven-field prostate IMRT plan. The percentage of γ ≤ 1 within the 20% isodose line for each field is given in brackets

measurements and the TPS agreed within the γ criteria of 3% and 3 mm for at least 93.3% of the points within the 20% isodose surface. We assumed that the linear accelerator (Linac) settings, such as, the number of monitor units and MLC parameters, were accurately transferred from the TPS to the treatment machine. Moreover, it proved that for a homogenous object, the 2D dose-reconstruction algorithm based on EPID transmission images was accurate within the γ criteria of 3% and 3 mm. Note that the dose verification for a 10×10 cm^2 field was completely satisfied based on the 3%/3 mm criteria [Table 1]. A similar observation was made by Wendling *et al*.[5] On account of the excellent agreement between reconstructed and calculated dose values in the homogenous phantom, the 2D EPID dosimetry algorithm could potentially be extended for situations where inhomogeneities, such as air cavities, were present, for example, in an anthropomorphic phantom or patient (*in vivo* EPID-based dosimetry). To illustrate that the 2D *in vivo* EPID dosimetry algorithm in the presence of inhomogeneties was more useful than a pretreatment verification using a phantom or a fluence check, in-Alderson phantom measurements were performed. *In vivo* EPID dosimetry did not test

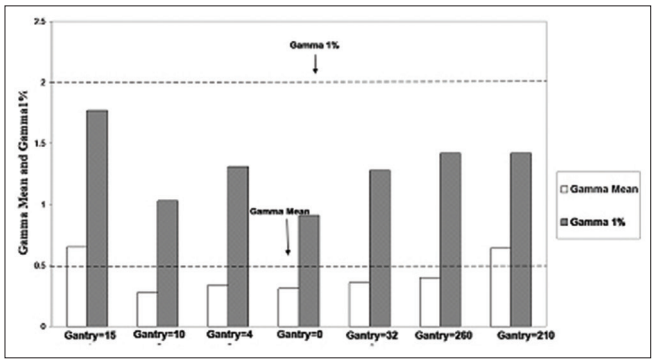

Figure 5: γ mean and γ1% results of a seven-field prostate IMRT plan. The dashed lines indicate the tolerance level

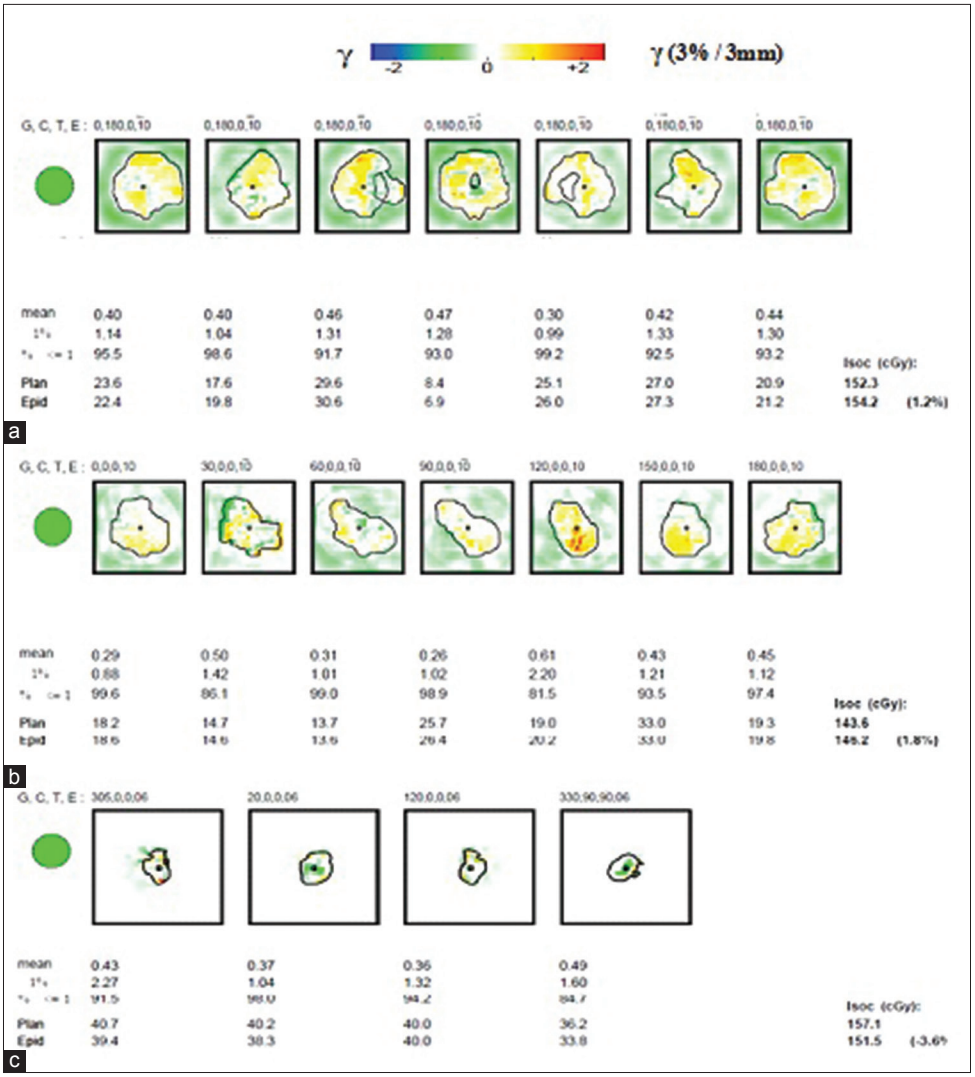

Figure 6: *In vivo* EPID dosimetry reports of the (a) prostate, (b) lung, and (c) head-and-neck plans. The symbols above the report indicate the gantry angle (G), collimator angle (C), table position (T), and beam energy (E)

Table 1: The results of γ-evaluation parameters and the measured/calculated dose difference at the isocenter for the box field in a homogenous slab phantom

Gantry angle(°)	Mean γ	γ1%	Dose difference at isocenter measured-calculated(%)
0	0.48±0.09	1.1±0.0	−2.5±0.7
90	0.41±0.12	1.0±0.2	−2.2±1.3
180	0.33±0.12	0.8±0.1	−0.5±1.6
270	0.38±0.11	1.0±0.1	−1.4±1.7

the inhomogenity correction of the TPS; the results showed that for the dose verification by Alderson phantom, the dose distributions resulting from the EPID measurements and the TPS agreed within the γ criteria of 3% and 3 mm. Moreover, most of the mean γ values were less than 0.5, except for the lung plan in the AP beam, the head-and-neck plan in the PA beam, and the IMRT prostate plan, only for the gantry angle of 210°. In case of the IMRT prostate plan, this discrepancy for a seven-field was ignorable and for the 3D conformal plans (the lung plan in the AP beam and the head-and-neck plan in the PA beam) it might be due to a larger sensitivity for setup variations and patient anatomy changes of the lung and head-and-neck plans, as compared to the prostate plan. Another reason might be that the use of a calculated transmission introduced an additional uncertainty.[30]

By looking in the EPID-based *in vivo* dosimetry reports [Figure 6], it can be seen that for the *in vivo* dose verifications, the EPID-based dose values differ only to a small extent from the planned dose values, for the head-and-neck case. There are several possible explanations why this deviation has occurred. First, the uncertainty of the reconstructed dose, in a low-dose, low-gradient region, using the back-projection algorithm is1.6% (1SD), which has been determined by repeating a measurement for a head-and-neck case for over a nine-month period, at different accelerators. Furthermore, some of the segments are very irregular in shape in the high-dose regions. The other data presented in Figure 6 illustrate that the 2D EPID-based dosimetry algorithm is accurate in dose verification for at least the prostate, head-and-neck, and lung plans, however, further investigation to improve the 2D EPID dosimetry algorithm for the head-and-neck case, is necessary. The accuracy of the 2D-EPID based *in vivo* dosimetry algorithm is in agreement with the observations reported by McDermott *et al*.[15] Moreover, the advantages of *in vivo* dosimetry are that a check and record of the actual treatment is obtained in the measurement time, without additional cost. This is only an advantage if the method can be shown to be as accurate, and provide as much information as necessary, during pretreatment dosimetry. The number of measured *in vivo* fractions required to replace pretreatment verification is a balance between early detection and workload. Another big advantage of *in vivo* EPID dosimetry is that the workload of treatments is considerably reduced compared to the pretreatment verification.[15] The only aspect that is not verified in this approach is the accuracy of the TPS tissue inhomogenity correction (including the correct selection of the CT density table). We assume that the TPS tissue inhomogenity correction is checked during the commissioning process of the TPS and that for the correct selection of the CT density tables, other QA procedures are required. Other groups have used advanced dose calculation algorithms such as the Monte Carlo methods, for EPID-based dose verification.[31] These approaches also give accurate results within the inhomogeneous tissue regions such as the lung. However, the use of these methods is counterbalanced by their complexity and the considerably longer time needed for dose calculation.

CONCLUSION

We have shown that a 2D EPID-based dosimetry algorithm provides an accurate method to verify the dose of simple 10 × 10 cm^2 fields inside a homogenous slab phantom, as well as the IMRT prostate plan and 3D conformal plans (prostate, head-and-neck, and lung plans) inside the anthropomorphic phantom. The model for 2D *in vivo* dose reconstruction from EPID images for 3D conformal treatments of a prostate, a head-and-neck, and a lung cancer patient is accurate within the γ criteria of 3% and 3 mm inside the patient, when the external patient contour is known. The algorithm is fast and is independent of the TPS. It provides a safety net for patient treatment.

ACKNOWLEDGMENT

The authors would like to thank the Department of Radiation Oncology, the Netherlands Cancer Institute-Antoni van Leeuwenhoek Hospital (NKI-AVL) and Rene Tielenburg for their help with measurements. This study was financially supported by the Ministry of Health and Medical Education of Iran.

REFERENCES

1. Steinke MF, Bezak E. Technological approaches to in-room CBCT imaging. Australas Phys Eng Sci Med 2008;31:167-79.
2. vanHerk M. Different styles of image-guided radiotherapy. Semin Radiat Oncol 2007;17:258-67.
3. Dawson LA, Jaffray DA. Advances in image-guided radiation therapy. J Clin Oncol 2007;25:938-46.
4. Mans A, Wendling M, McDermott LN, Sonke JJ, Tielenburg R, Vijlbrief R, *et al*. Catching errors with *in vivo* EPID dosimetry. Med Phys 2010;37:2638-44.

5. Wendling M, Louwe RJ, McDermott LN, Sonke JJ, van Herk M, Mijnheer BJ. Accurate two-dimensional IMRT verification using a back-projection EPID dosimetry method. Med Phys 2006;33:259-73.
6. Kirby MC, Glendinning AG. Developments in electronic portal imaging systems. Br J Radiol 2006;79:S50-65.
7. Kaatee RS, Olofsen MJ, Verstraate MB, Quint S, Heijmen BJ. Detection of organ movement in cervix cancer patients using a fluoroscopic electronic portal imaging device and radiopaque markers. Int J Radiat Oncol Biol Phys 2002;54:576-83.
8. Mohammadi M, Bezak E. The physical characteristics of a SLIC-EPID for transmitted dosimetry. Int J Radiat Res 2005;2:175-83.
9. Nijsten SM, Mijnheer BJ, Dekker AL, Lambin P, Minken AW. Routine individualised patient dosimetry using electronic portal imaging devices. Radiother Oncol 2007;83:65-75.
10. Erridge SC, Seppenwoolde Y, Muller SH, van Herk M, De Jaeger K, Belderbos JS, *et al*. Portal imaging to assess set-up errors, tumor motion and tumor shrinkage during conformal radiotherapy of non-small cell lung cancer. Radiother Oncol 2003;66:75-85.
11. Hurkmans CW, Remeijer P, Lebesque JV, Mijnheer BJ. Set-up verification using portal imaging; review of current clinical practice. Radiother Oncol 2001;58:105-20.
12. Van den Heuvel F, Fugazzi J, Seppi E, Forman JD. Clinical application of a repositioning scheme, using gold markers and electronic portal imaging. Radiother Oncol 2006;79:94-100.
13. Bogaerts R, Van Esch A, Reyman R, Huyskens D. A method to estimate the transit dose on the beam axis for verification of dose delivery with portal images. Radiother Oncol 2000;54:39-46.
14. McDermott LN, Wendling M, van Asselen B, Stroom J, Sonke JJ, van Herk M, *et al*. Clinical experience with EPID dosimetry for prostate IMRT pre-treatment dose verification. Med Phys 2006;33:3921-30.
15. McDermott LN, Wendling M, Sonke JJ, van Herk M, Mijnheer BJ. Replacing pretreatment verification with *in vivo* EPID dosimetry for prostate IMRT. Int J Radiat Oncol Biol Phys 2007;67:1568-77.
16. McDermott LN, Wendling M, Nijkamp J, Mans A, Sonke JJ, Mijnheer BJ, *et al*. 3D *in vivo* dose verification of entire hypo-fractionated IMRT treatments using an EPID and cone-beam CT. Radiother Oncol 2008;86:35-42.
17. Van Elmpt W, McDermott L, Nijsten S, Wendling M, Lambina P, Mijnheer B. A literature review of electronic portal imaging for radiotherapy dosimetry. Radiother Oncol 2008;88:289-309.
18. Pasma KL, Dirkx ML, Kroonwijk M, Visser AG, Heijmen BJ. Dosimetricverification of intensity modulated beams produced with dynamic multileaf collimation using an electronic portal imaging device. Med Phys 1999;26:2373-8.
19. McNutt TR, Mackie TR, Reckwerdt P, Papanikolaou N, Paliwal BR. Calculation of portal dose using the convolution/superposition method. Med Phys 1996;23:527-35.
20. Huyskens D, Van Dam J, Dutreix A. Midplane dose determination using *in vivo* dose measurements in combination with portal imaging. Phys Med Biol 1994;39:1089-101.
21. Terrón JA, Sánchez-Doblado F, Arráns R, Sánchez-Nieto B, Errazquin L. Midline dose algorithm for *in vivo*dosimetry. Med Dosim 1994;19:263-7.
22. Rizzotti A, CompriC, Garusi GF. Dose evaluation to patients irradiated by 60Co beams, by means of direct measurement on the incident and on the exit surfaces. Radiother Oncol 1985;3:279-83.
23. Boellaard R, Essers M, van Herk M, Mijnheer BJ. New method to obtain the midplane dose using portal *in vivo*dosimetry. Int J Radiat Oncol Biol Phys 1998;41:465-74.
24. Jordan TJ, Williams PC. The design and performance characteristics of a multileaf collimator. Phys Med Biol 1994;39:231-51.
25. McDermott LN, Louwe RJ, Sonke JJ, van Herk MB, Mijnheer BJ. Dose-response and ghosting effects of an amorphous silicon electronic portal imaging device. Med Phys 2004;31:285-95.
26. Louwe RJ, McDermott LN, Sonke JJ, Tielenburg R, Wendling M, van Herk MB, *et al*. The long-term stability of amorphous silicon flat panel imaging devices for dosimetry purposes. Med Phys 2004;31:2989-95.
27. Boellaard R, van Herk M, Uiterwaal H, Mijnheer B. First clinical tests using a liquid-filled electronic portal imaging device and a convolution model for the verification of the midplane dose. Radiother Oncol 1998;47:303-12.
28. Louwe RJ, Damen EM, van Herk M, Minken AW, Törzsök O, Mijnheer BJ. Three-dimensional dose reconstruction of breast cancer treatment using portal imaging. Med Phys 2003;30:2376-89.
29. Wendling M, McDermott LN, Mans A, Olaciregui-Ruiz Í, Pecharromán-Gallego R, Sonke JJ, *et al*. In aqua vivo EPID dosimetry. Med Phys 2012;39:367-77.
30. Pecharromán-Gallego R, Mans A, Sonke JJ, Stroom JC, Olaciregui-Ruiz I, van Herk M, *et al*. Simplifying EPID dosimetry for IMRT treatment verification. Med Phys 2011;38:983-92.
31. vanElmpt WJ, Nijsten SM, Dekker AL, Mijnheer BJ, Lambin P. Treatment verification in the presence of inhomogeneities using EPID-based three-dimensional dose reconstruction. Med Phys 2007;34:2816-26.

Source of Support: Nil, **Conflict of Interest:** None declared.